

# The behavior of lightweight aggregate concrete filled steel tube columns under eccentric loading

Elzien Abdelgadir\*, Ji Bohai, Fu Zhongqiu, and Hu Zhengqing

College of Civil Engineering, Hohai University, Nanjing 210098, China

(Received July 16, 2010, Revised May 07, 2011, Accepted August 17, 2011)

**Abstract.** This paper consists of two parts; the first part describes the laboratory work concerning the behavior of lightweight aggregate concrete filled steel tubes (LACFT). Based on eccentricity tests, fifty-four specimens with different slenderness ratios ( $L/D=3, 7, \text{ and } 14$ ) were tested. The main parameters varied in the test are: load eccentricity; steel ratio; and slenderness ratio. The standard load-strain curves of LACFT columns under eccentric loading were summarized and significant parameters affecting LACFT column's bearing capacity, failure mechanism and failure mode such as confinement effect and bond strength were all studied and analyzed through the comparison with predicted strength of concrete filled steel tube columns (CFT) using the existing codes such as AISC-LRFD (1999), CHN DBJ 13-51-2003 (2003) and CHN CECS 28:90 (1990). The second part of this paper presents the results of parametric study and introduces a practical and accurate method for determination of the maximum compressive strength of confined concrete core ( $f_{\max}$ ). In addition to, the study of the effect of aspect-ratio and length-width ratio on the yield stress of steel tubes ( $f_{sy}$ ) under biaxial state of stress in CFT columns and the effect of these two factors on the ultimate load carrying capacity of axially loaded CFT/LACFT columns.

**Keywords:** lightweight aggregate concrete filled steel tube; load eccentricity; steel ratio; slenderness ratio; ultimate bearing capacity; composite construction

---

## 1. Introduction

In concrete construction, self-weight represents a very large proportion of the total load on the structure, and there are clearly considerable advantages in reducing the density of concrete. One of the ways to reduce the mass or dead weight of a structure is the use of composite construction. A second way is by the use of lightweight aggregate in concrete to get lightweight aggregate concrete (LAC).

Composite construction; consists of using more than one material in structural units, and at the same time using each material to its best advantage. Concrete filled steel tubes (CFT) as a composite material have been used widely in structures throughout the world in recent years. This increase in use of CFT is due to the large number of studies carried out on CFT columns (Furlong 1967, Knowles 1969, Ge and Usami 1992, 1994, Boyd *et al.* 1995, Bradford 1996, Shams and Saadeghvaziri 1997, Hajjar *et al.* 1998, Schneider 1998, Kitada 1998, Roedr *et al.* 1999, Zhang and Shahrooz 1999, Uy 2000, O'Shea and Bridge 2000, Elchalakani *et al.* 2001, Bradfor *et al.* 2002, Elremaily 2002, Huang *et al.* 2002, Hu *et al.* 2003), In addition to the significant advantages that CFT offers in comparison to others traditional

\* Corresponding author, Ph. D., Student, E-mail: [drsha82@hhu.edu.cn](mailto:drsha82@hhu.edu.cn)

methods. The benefit of lightweight aggregate in concrete as structural material has been recognized as far back as Roman days. Although there is few published data available on the researches of the LACFT but several authors [Ji *et al.* 2010, Zuobin and Xiliang 1993, Mouli and Khelafi 2007] in their investigations reported that LAC has its obvious advantages of higher strength/weight ratio, lightweight, good ductility, convenience of construction, lower coefficient of thermal expansion, and superior heat and sound insulation characteristic due to air voids in the lightweight aggregate. The reduction in dead weight of construction by the use of lightweight aggregate concrete could result in a decrease in cross section of columns, beams, plates, and foundations and construction costs. Lightweight aggregate concrete filled steel tube (LACFT) as a new form of composite structures, under the same conditions, not only has the same strength and durability as the CFT, but also reduces the deadweight of the structure by about 20%.

Nowadays, with the trend towards large-span bridges and towering direction of building structures, the LACFT with its distinguished characteristics, will have broad applications prospects. In recent years, studies are focused on CFT or high-strength concrete filled steel tube and some of these studies results have been theorized (Shantung 2003, Sumei and Yuning 2004), however, structural studies on LACFT are still in the initial step all over the world.

Because of CFT component's advantages of high compression strength and good plastic deformation, often used as a compression member, applied in bridge engineering such as the arch rib of pier or arch bridge. Nevertheless, in the practice of actual engineering the influence of the initial defects, material in homogeneity, manufacturing deviations and other factors, on the ideal axial compression is very difficult to avoid. At the same time the multistory and high-rise buildings under the act of the vertical load, lateral horizontal wind or seismic forces, will also be bore by the moment, hence the component tends to the state of eccentric compression (Han and yang 2004). Consequently, the study of eccentric compression of LACFT will have important and significance role in the theoretical researches and engineering applications value. Based on eccentricity tests, fifty-four specimens with different slenderness ratios ( $(L/D) = 3, 7$  and  $14$ ) were tested. The main parameters varied in the tests are: (1) load eccentricity; (2) steel ratio; and (3) slenderness ratio. The standard load-strain curves of LACFT columns under eccentric loading were summarized and significant parameters affecting LACFT column's bearing capacity, failure mechanism and failure mode were all studied and analyzed through the comparison with predicted strength of CFT columns using the existing codes such as AISC-LRFD (1999), CHN DBJ 13-51-2003 (2003) and CHN CECS 28:90 (1990).

## 2. Test arrangement and procedure

### 2.1. Specimens and material

The coarse aggregate of the lightweight aggregate concrete in the test is fly ash - shale ceramic with physical and mechanical properties as follow: Lightweight aggregate of Bulk density  $814 \text{ kg/m}^3$ , and cylindrical compressive strength  $8.5 \text{ MPa}$  with water absorption ratio 6% an hour. The concrete mix proportion and mechanical properties are given in Table 1. The mix prepared by using the agitator and simple curing techniques. In accordance to the relevant Chinese standards; compression tests were carried out on a number of Standard cubes ( $150 \times 150 \times 150 \text{ mm}$ ) to determine the concrete grade and prisms ( $150 \times 150 \times 300 \text{ mm}$ ) in order to determine the 28-days compressive strength ( $f_{ck}$ ) and Young's modulus ( $E_c$ ) of the unconfined concrete.

Table 1 The mixture ratios and mechanical properties of lightweight aggregate concrete

Component	Mix parameters
Cement content	460 kg/m <sup>3</sup>
Ceramisite	670 kg/m <sup>3</sup>
Sand	650 kg/m <sup>3</sup>
Water	150 kg/m <sup>3</sup>
Concrete bulk density	1810 kg/m <sup>3</sup>
Characteristic 28-days concrete cube strength	44.7 MPa
Characteristic 28-days concrete prism strength $f_{ck}$	35.2 MPa
the Young's Modulus of concrete $E_c$	26.2 GPa

Straight welded steel tube Q235 was used in this experiments. According to the Chinese standard “Metallic materials at ambient temperature tensile test method” (GB/T228-2002) (2002); tension tests on a group of three were conducted to determine tensile strength, where the thickness of each section of steel tube made into the interception of the standard specimen. Before pouring concrete, each column was welded with a 10 mm thick and a diameter slightly larger than the steel tube circular plate on one side then 20.5 mm diameter hole was created as aperture in the center of the plate. The LAC was filled in layers; each layer was 500 mm vibrated manually to ensure its density, and cured by natural conditions. Surface hollows due to concrete shrinkage were filled up with grout to confirm the specimen side smoothness and after 24-hours of treatment; another circular plate was welded on the other side. The parameters of LACFT specimens and the test results are given in Table 2.

## 2.2. Test instruments and test procedure

The details of the test instruments are shown in Fig. 1. The experiment was run in the structural engineering laboratory of Hohai University. Hydraulic jack was implemented to apply loads on the specimens. Pressure sensor and resistance strain gauges were installed to measure loads and strains respectively. At the two ends of the specimen utilized column joint to simulate the hinged boundary conditions.

For the safety and accuracy of the specimen tests, three round holes of 20 mm diameter and 15 mm depth were set according to the 10 mm, 20 mm, 35 mm eccentric distances far from the center, of the bottom column roller. During the test a steel rabbet with a diameter of 20 mm and 25 mm length was used to connect specimen's plate with the column joint. For the accuracy of the specimen's deformation measurements, eight strain gauges were setup up at the mid-length of the column to record strains values. In the bending plane three displacements meters were installed, the top and the bottom gauges were at distance of one fourth the height of each column from the top and the bottom respectively and the third displacement gauge was positioned at the mid-height of each column to measure the lateral deformation. In order to measure the portrait deformation two displacements gauges were setup. All these gauges were connected to a computer data acquisition system to record their values in the whole test phases.

The specimens were loaded at rate of 1/10 of the predicted ultimate load in the elastic phase and at loading rate of 1/15 of the predicted ultimate load in the column yielding phase. Every load was maintained two-three minutes to enable the full deformation development. When approaching the

Table 2 Details of the test specimens

columns	Size $D \times t \times L$ (mm)	Eccentricity distances $e_0$ (mm)	Steel ratio $\alpha$ (%)	L/D	$f_y$ (MPa)	$f_{ck}$ (MPa)	Ultimate strength $N_u$ (kN)	Reduction factor of loading $\phi$
A1-3-a	114 × 3 × 342	10	11.4	3	274.7	35.2	685.04	0.841
A1-3-b							670.07	
A1-3-c							696.35	
A2-3-a	114 × 3 × 342	20	11.4	3	274.7	35.2	564.23	0.688
A2-3-b							541.24	
A2-3-c							573.72	
A3-3-a	114 × 3 × 342	35	11.4	3	274.7	35.2	424.45	0.519
A3-3-b							430.29	
A3-3-c							411.31	
B1-3-a	114 × 3.5 × 342	10	13.5	3	274.7	35.2	714.60	0.842
B1-3-b							753.65	
B1-3-c							762.04	
B2-3-a	114 × 3.5 × 342	20	13.5	3	274.7	35.2	595.26	0.694
B2-3-b							626.64	
B2-3-c							616.42	
B3-3-a	114 × 3.5 × 342	35	13.5	3	274.7	35.2	447.08	0.505
B3-3-b							447.81	
B3-3-c							442.70	
A1-7-a	114 × 3 × 798	10	11.4	7	274.7	35.2	554.38	0.724
A1-7-b							602.55	
A1-7-c							609.85	
A2-7-a	114 × 3 × 798	20	11.4	7	274.7	35.2	442.34	0.555
A2-7-b							467.15	
A2-7-c							444.61	
A3-7-a	114 × 3 × 798	35	11.4	7	274.7	35.2	329.56	0.407
A3-7-b							329.20	
A3-7-c							333.21	
A1-14-a	114 × 3 × 1596	10	11.4	14	274.7	35.2	533.94	0.652
A1-14-b							537.96	
A1-14-c							518.98	
A2-14-a	114 × 3 × 1596	20	11.4	14	274.7	35.2	401.82	0.506
A2-14-b							415.69	
A2-14-c							416.42	
A3-14-a	114 × 3 × 1596	35	11.4	14	274.7	35.2	315.33	0.383
A3-14-b							312.42	
A3-14-c							306.20	
B1-7-a	114 × 3.5 × 798	10	13.5	7	274.7	35.2	618.98	0.705
B1-7-b							616.42	
B1-7-c							633.58	
B2-7-a	114 × 3.5 × 798	20	13.5	7	274.7	35.2	405.84	0.521
B2-7-b							486.50	
B2-7-c							489.05	
B3-7-a	114 × 3.5 × 798	35	13.5	7	274.7	35.2	382.12	0.422
B3-7-b							370.80	
B3-7-c							366.42	
B1-14-a	114 × 3.5 × 1596	10	13.5	14	274.7	35.2	579.20	0.625
B1-14-b							486.86	
B1-14-c							589.78	
B2-14-a	114 × 3.5 × 1596	20	13.5	14	274.7	35.2	452.55	0.518
B2-14-b							448.54	
B2-14-c							470.80	
B3-14-a	114 × 3.5 × 1596	35	13.5	14	274.7	35.2	346.35	0.394
B3-14-b							342.34	
B3-14-c							355.47	

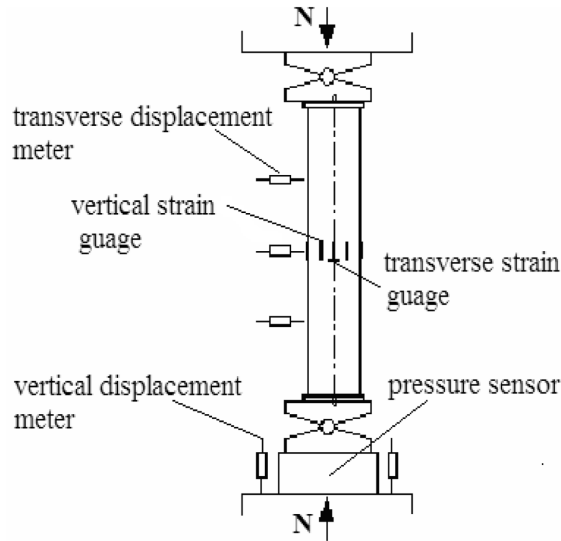


Fig. 1 Loading and measurement system

ultimate load, slow loading mode was applied. Any one of two conditions concluded the test: (1) the maximum deformation reached, (2), or obvious features of failure occurred in the specimens.

### 2.3. Results of the test and analysis

#### 2.3.1. Experimental phenomena and failure mode

Specimens have shown Different failure modes illustrated in Fig. 2. This figure gives a general view of the specimens after test. When the load was small, the lateral deflection of the specimen at middle height was small and approximately proportional to the applied load. But when the load reached about 60-70% of the maximum load, the lateral deflection at middle height started to increase significantly. It can be seen that, generally, for the circular specimens filled with LAC, Typical failure modes of HSS columns filled with LAC concrete were all overall buckling. During the test, the deflection curve was approximately in the shape of a half sine wave. Fig. 3 illustrates the lateral deflection development of the composite columns with different axial load level near the center before and after peak load. The sinusoids with the same values in the middle height are also shown in Fig. 3 using dashed lines. This indicates the validity of the assumption of 'the deflection curve of the member is a half sine wave', which is adopted in the literature (Han and Yao and 2003, Han *et al.* 2001). In general the failure mode of the specimens was a function of the  $L/D$  and  $D/t$  ratios and also of load eccentricity ratios. The short columns ( $L/D = 3$ ) failed due to the crushing of the concrete core, aggravated by the local buckling of steel tube after having reached the yielding stress of the steel tube Fig. 2(a). It should also be noted that concrete fracture was observed on the tension side of some specimens with  $L/D > 3$  under large deformation but no local buckling was observed Fig. 2(b), 2(c). It was observed that columns with  $D/t = 33$  can better restrain the expansion of the concrete core than the columns with  $D/t = 38$  for the same concrete compressive strength (35.2 Mpa). It was also noticed the increase in the lateral strain in columns is uniform along the height, where the lateral strain is more localized at the middle height. No local buckling was found in the compression zone of a steel tube before achieving the ultimate strength.

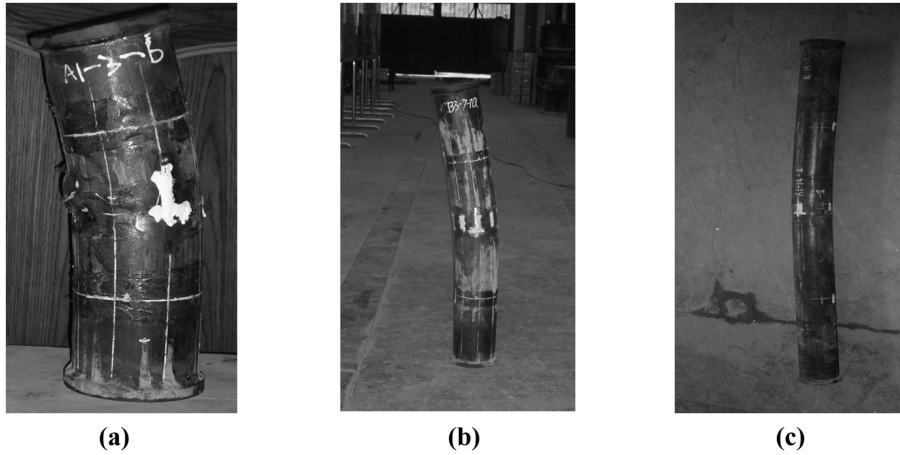


Fig. 2 Typical failure modes of specimens

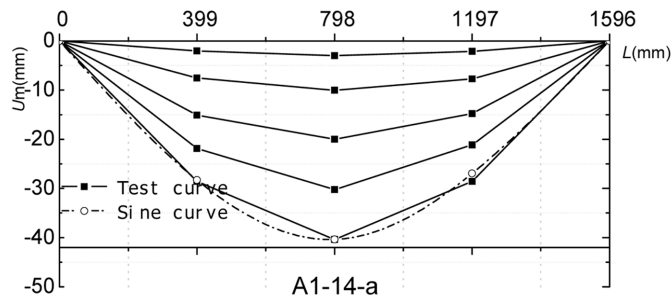


Fig.3 Deflection positions along the length measured with the displacement meters

The axial load (N) versus extreme longitudinal fiber tensile and compressive strain relationships are shown in Fig. 4. It can be seen that LACFT columns show similar behavior to that reported by Yang and Han (2006). In general, the strain corresponding to the ultimate strength increases with the increase of the load eccentricity ratio. For circular specimens, the compressive strain corresponding to the ultimate strength exceeds the steel yielding strain ( $1,700 \mu\epsilon$ ). Strain distribution Curves of the specimens middle section for three different eccentric ratios are shown in Fig. 4, where “+” and “-” signs represents compressive and tensile strains respectively. From the Figure it is observed, the section deformation of specimen's agree with the plane section assumption in each loading stage. Level of correspondence for plane section at initial loading stage was better than later loading stages. For small eccentric ratios, neutral axis location moved gradually to the load location along with load increasing, but it was unobvious for large eccentric ratios. By referring to the data published by Yang and Han (2006) it is possible to conclude that the features of LACFT columns are generally similar to those of CFTs regardless to the type of concrete.

### 2.3.2. Analysis of failure course

The load–strain curves of LACFT are shown in Fig. 5. According to this figure, at elastic phase the

The Behavior of Lightweight Aggregate Concrete Filled Steel Tube Columns Under Eccentric Loading

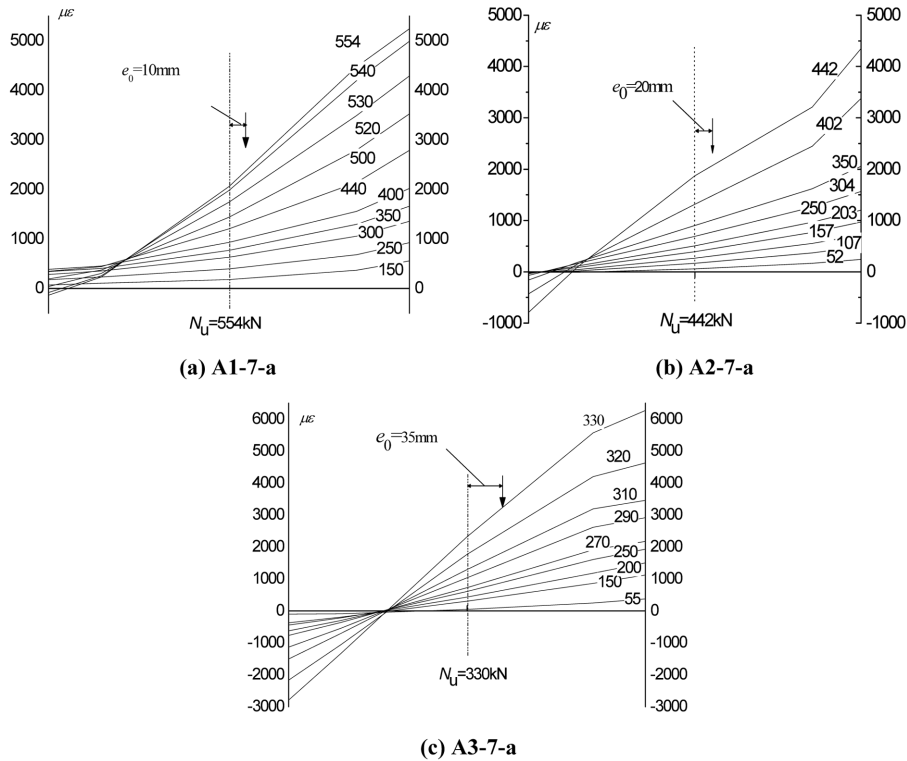


Fig. 4 Curve of strain distribution by different eccentric ratio

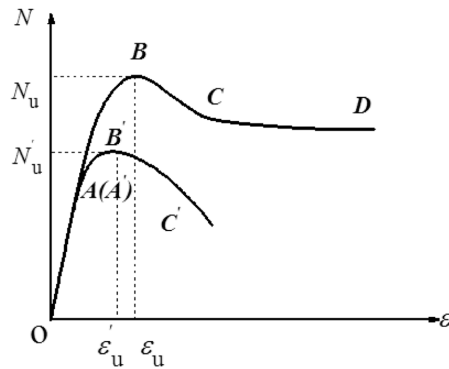


Fig. 5 Sketch map of  $N$ - $\varepsilon$  curves

curves (OA and O'A') of the columns with  $L/D \leq 3$  and  $L/D > 3$  are similar and approximated linearly. It is clear that all the curves of various samples are almost coincidence at this phase. The proportional limit load (A and A') is 60% to 70% of the ultimate load. As the load increase, the curves gradually deviates from straight line and enters into the elastic-plastic stage (AB and A'B'), simultaneously the compression zone of steel tube begins to yield, the concrete core was cracked and the lateral deflection

of all specimens became larger. At the ultimate load, the curves enters into the declining stage (BC and B'C'), where the bearing capacity decreased with the increment of the lateral deflection, and the curve declined more tardily.

It is observed that the LACFT columns have been able to maintain greater capacity, and good ductility performance, simultaneous with various degrees of partial bending drum appeared on the surface of the steel tube; hence filled with lightweight aggregate concrete can effectively delay the deflections of steel tube. The curves of columns ( $L/D > 3$ ) have showed that the larger eccentricity ratio is the larger longitudinal strain would be. Therefore large overall deformation and lateral buckling were occurred in specimens.

2.3.3. Analysis of failure mechanism

Fig. 6 illustrates Poisson's ratio ( $\nu$ ) of the composite materials versus bearing capacity in different regions of the cross-section. This ratio is usually 0.25 to 0.3, and the average one is 0.283. Generally, when Poisson's ratio of the composite materials is more than the steel tube Poisson's ratio; steel tube breeds a constraint effect on the concrete (Han and yang 2004). From Fig. 6, in the initial stage of loading, Poisson's ratio in the regional cross-section of steel tube mainly maintain about 0.2 to 0.3, therefore, the constraint effect of steel tube on the concrete is smaller. In the elastic-plastic phase, at the edge of the compression zone the Poisson's ratio significantly increased close to the ultimate load, at the same time gradual increase occurred at the symmetry axis, but at the edge of the tension section the ratio preserve unchanged or with a little change.

Hence circular steel tubes under eccentric load are able to generate the constraint effect on the core concrete. Also found, the larger Poisson's ratio is, the stronger confinement effect on the core LAC caused by the steel tube is.

3.1. The influencing parameters of the columns

3.1.1. Influence of eccentricity ratio

It was found that eccentricity ratio is a significant parameter to the mechanical properties of LACFT columns. To analyze the relation of eccentricity ratio versus bearing capacity of the columns under eccentric axial compression load, stress-strain curves of different specimens which have similar steel

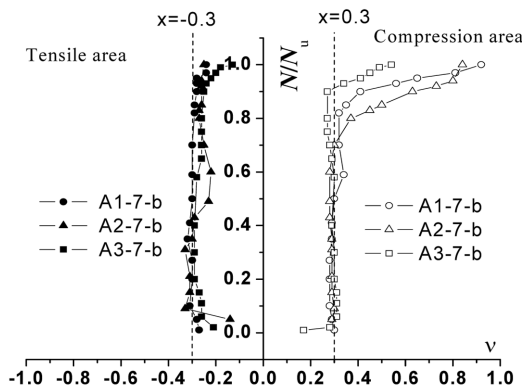


Fig. 6  $N/N_u$  versus Poisson's ratio ( $\nu$ ) of the composite material in the cross-section of mid-span

and concrete characteristic properties but with various eccentric ratios were visualized in Fig. 7. The figure has shown that as a result of the influence of large eccentricity; the bearing capacity and rigidity decreased, while the ductility performance effectively improved. As a conclusion could be argued that; the greater the eccentricity ratio, the less the ultimate bearing capacity, therefore the constraint effects in this case has less impact on the improvement of bearing capacity of the LACFT columns.

### 3.1.2 Influence of steel ratio

The steel's ratio influence on the specimen's bearing capacity performance is shown in Fig. 8; In the early stage of loading and by using different ratios of steel and various eccentricities, the load versus deformation curves in the middle of columns have shown approximately similar slope (Fig. 8(a), (c)). But in a later stage of loading, these curves showed a clear separation (Fig. 8(b), (d)). Thus, the greater the steel ratio, the greater the ascending slope of the curves, as well as increased the ultimate bearing capacity. This phenomenon can be explained as a result of the confinement growing effect on the LAC

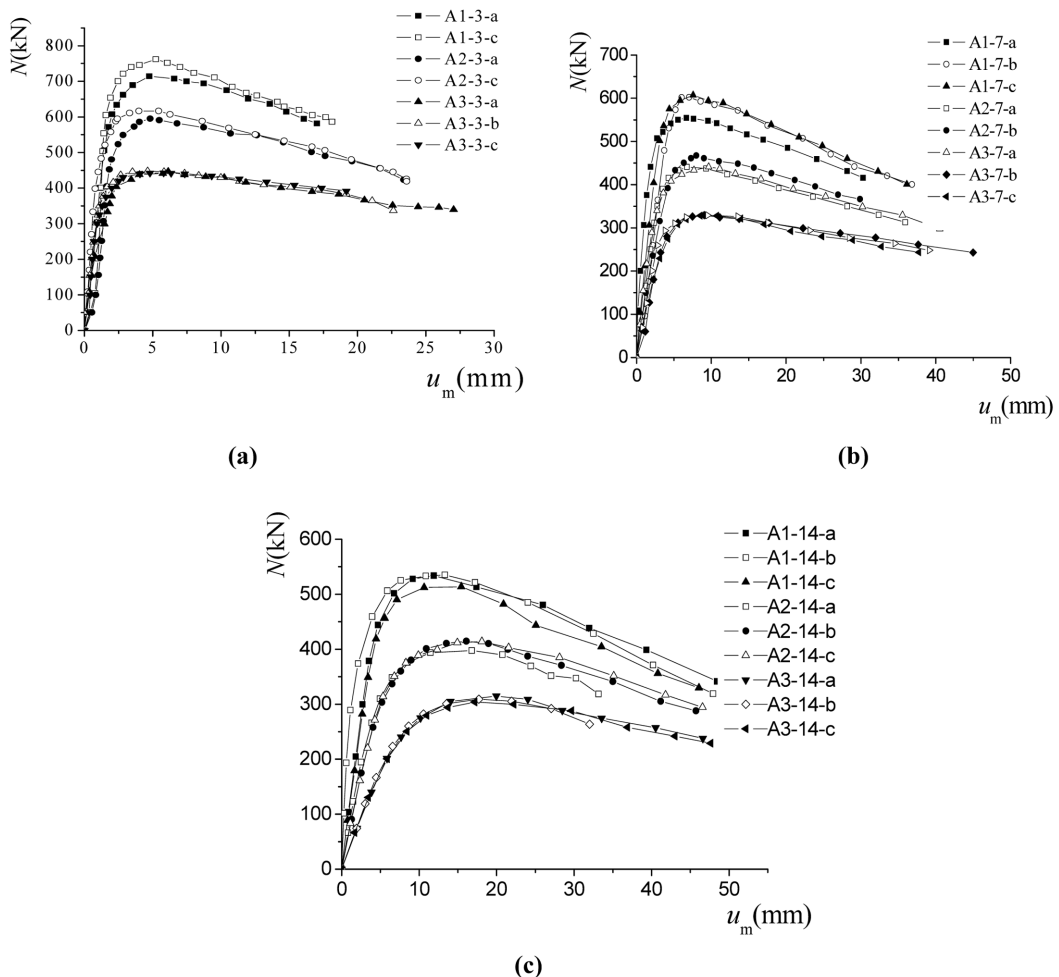


Fig. 7  $N$ - $u_m$  relationship curves of specimen with different eccentricity ratios

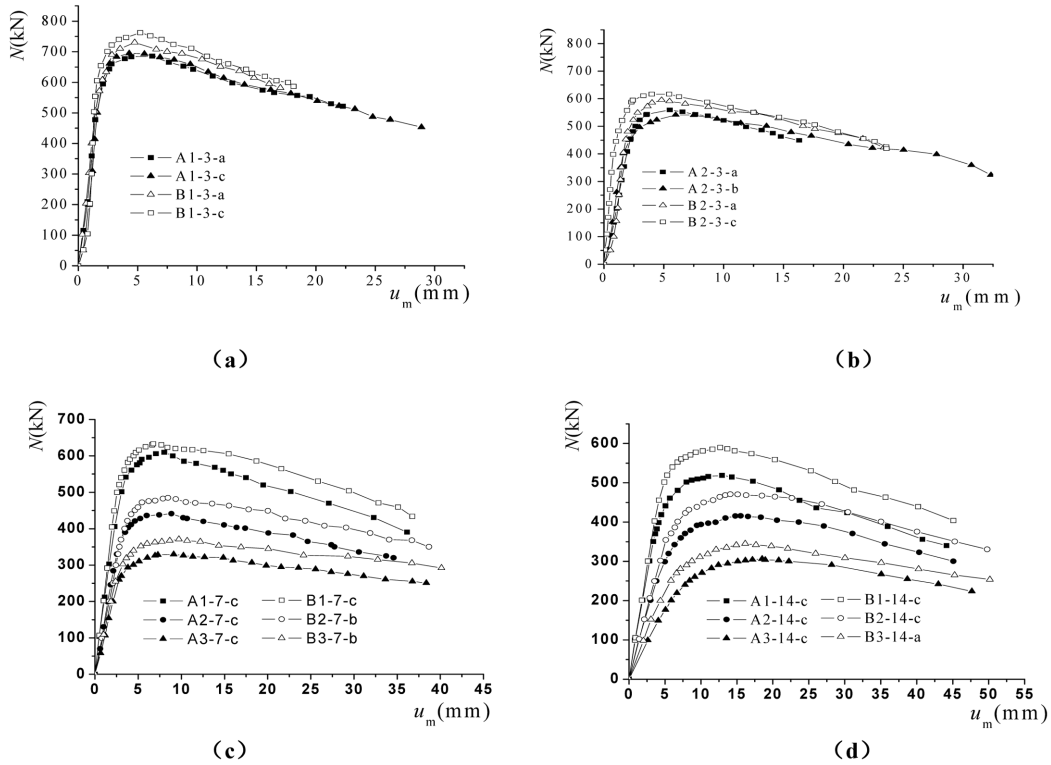


Fig. 8 N- $u_m$  relationship curves of specimen with different steel ratio

core which is gained by increasing steel ratio, which enhanced specimen's strength by developing additional moment of resistance in the compression zone, together with the progress of Poisson's ratio. From Table 3 it can be seen that when steel ratio was increased from 11.4% to 13.5% resulted in an increase of the specimen ultimate bearing capacity about 8%.

### 3.2.3. Influence of slenderness ratio

The impact of slenderness ratio on the columns that have  $L / D > 3$  was investigated and shown in Fig. 9. At the initial loading stage, specimen's materials have displayed elastic behavior concurrent with small lateral deformation, and small additional moment caused by the lateral deformation under eccentric load. In elastic-plastic stage additional moment occurred, due to the growing of the specimen's longitudinal deformation as a result of slenderness ratio increasing, hence, smaller ascending slope and lower bearing capacity were achieved.

### 3.2.4. Confinement and bond effect

Although this section of the paper is not part of this research, it will be discussed as a complementary part to this article depending on the data available. It is well known that the level of increase in axial compressive strength by the confining effect of the steel tube depends on several factors, namely the thickness of the steel tube, slenderness ratio, eccentricity and cross-sectional shape. In literature there was an agreement that circular steel tube sections has significant confining effect on concrete core, and the lateral pressure is expected to distribute uniformly (Mander *et al.* 1988, Tomii 1988, Han *et al.* 2001)

Table 3 Bearing capacity formulas for concrete filled steel tubes

Number	References	Proposed formula	Notes
1	(AISC-LRFD 1999)	$\frac{N}{\varphi_c N_u} < 0.2, \quad \frac{N}{2\varphi_c N_u} + \frac{M}{\varphi_b N_u} \leq 1$ $\frac{N}{\varphi_c N_u} \geq 0.2, \quad \frac{N}{\varphi_c N_u} + \frac{8M}{9\varphi_b M_u} \leq 1$	United states norms AISC-LRFD(1999)
2	(DBJ13-51 2003)	$N/N_0 < 2\varphi^3\eta_0, \quad \frac{N}{\varphi N_u} + \frac{a}{d} \cdot \frac{\beta_m \cdot M}{M_u} \leq 1$ $N/N_0 \geq 2\varphi^3\eta_0, \quad \frac{-b \cdot N^2}{N_u^2} - \frac{c \cdot N}{N_u} + \frac{1}{d} \cdot \frac{\beta_m \cdot M}{M_u} \leq 1$	Formula included in norm CHN DBJ 13-51-2003 (2003)
3	(CECS 28:90 1990)	$e_o/r_c > 1.55, \quad \varphi_e = 0.4/(e_o/r_c)$ $e_o/r_c \leq 1.55, \quad \varphi_e = \frac{1}{1 + 1.85e_o/r_c}$ $\varphi_l = 1 - 0.115\sqrt{L_o/D - 4}$ $N = \varphi_l \cdot \varphi_e \cdot N_u$	Formula included in norms CHN CECS 28: 90

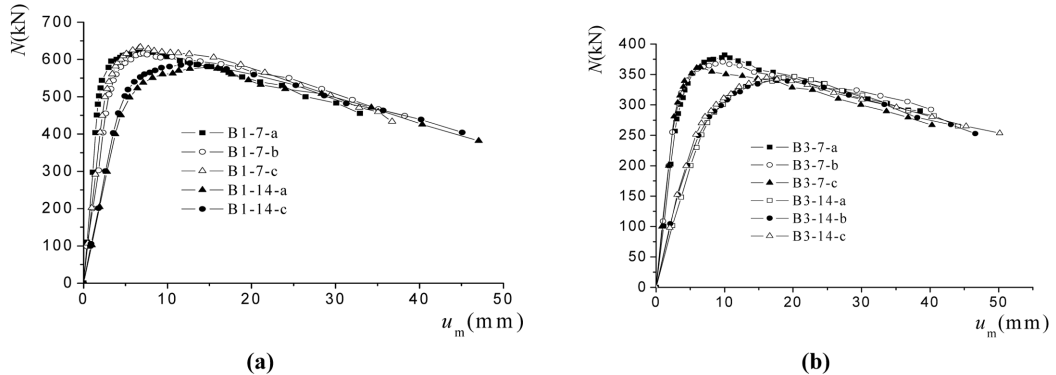


Fig. 9 Load versus deformation curves by different slenderness ratio

the confinement effect in columns under eccentric loading have also been investigated . Fujimoto T. *et al.* (2004) reported eccentric loading tests on 33 circular CFT Stub columns and stated that confinement effect is significant in circular columns. Ji *et al.*(2010) conducted tests on LAC columns under eccentric loading and found that steel tube can produce confinement on LAC concrete. However they also noted that the effectiveness of triaxial concrete confinement diminished as the axial load eccentricity increased. The authors also mentioned for  $L/D = 3$  without bending moment the squash load increased by up to 20% due to confinement effect. However Ji stated, with an eccentricity to diameter ( $e/D$ ) ratio of only 3% column strength increase due to confinement effect is reduced by about 29%. Liu and Song (2010) investigated the behavior of LAC and CFT specimens under multiaxial stresses and concluded

that the triaxial compressive strength of LAC is lower than that of normal concrete. Moreover they found the lightweight aggregate concrete under triaxial compression loads indicates a strength increase of about 20%-28% greater than the uniaxial compressive strength. In general the results found by Ji and Liu agree with each other and disagree with results published by Hunaiti *et al.* (2002), Hunaiti reported that there were no increase in axial capacity due to triaxial effects, but the tests results showed that LACFT behaved well under axial load and exhibited more ductility than bare steel tubes, also mentioned that the strength of composite short columns was enhanced and reached 70% of the strength of short columns filled with normal concrete. It is thus concluded that the features of LACFT columns are greatly similar to those of normal concrete (CFT).

Hunaiti (1996) performed push-out tests on concrete filled steel hollow sections of square and circular sections. The author mentioned that Bond strength between steel and concrete in composite sections depends on several factors. The shape of the cross section, the age, and the type of concrete were considered in this study. The test results reported that LAC showed higher resistance to push-out loads and thus better composite action. The author also noticed the strength of bond in tubes filled with LAC is about 30 to as much as 150% more than that in tubes filled with normal concrete. Moreover, bond reduction due to age in normal concrete specimens is higher than that in lightweight aggregate concrete specimens (28 and 90 days average bond strength in circular sections = 2.04, 1.37 MPa respectively). That was attributed partly to the larger aggregate content of the LAC, as well as the reserved moisture in the pumice aggregates and the expanded perlites, which probably compensate for the loss of water due to external drying, and thus reduce the shrinkage. The experimental results also show that the load-slip behavior of LAC specimens is similar to that of normal concrete filled specimens. There for it seems that when the slippage of the concrete core in the steel tube is prevented the bond strength does not have significant effect on the flexural capacity of CFT columns, therefore it can be neglected.

#### 4. Comparison and analysis of ultimate bearing capacity of columns

To evaluate the feasibility of currently available design codes in predicting the load bearing capacity of composite columns fabricated from lightweight aggregate concrete, the bearing capacities predicted using the following three design codes are compared with the current columns test results: AISC-LRFD (1999) (AISC-LRFD 1999), CHN DBJ 13-51-2003 (2003) and CHN CECS 28:90 of CFT.

In order to compare bearing capacity of LACFT columns subjected to eccentric compression with CFT ones under the same circumstances, the bearing capacity performance of fifty-four LACFT specimens was calculated by the formulas in Table 3. Table 4 shows the calculated values beside the measured one from experiment.

From Table 4, the calculated bearing capacities of LACFT referring to reference [AISC-LRFD 1999] are underestimated in compare to that of the test results, while the calculated value of CHN DBJ 13-51-2003 (2003) are applicable to predict the members bearing capacity, but the values predicted by CHN CECS 28:90 have a good agreement with experimental results.

In present it has not yet launched a calculation formula for the LACFT column's bearing capacity; therefore, the purpose of the code comparisons in this paper is only to evaluate the feasibility of these codes on lightweight aggregate concrete filled steel tube columns. According to the predicted results it is possible to say the formulas of the codes (AISC-LRFD 1999), (DBJ13-51 2003) and (CECS 28:90 1990) can be adopted to estimate the eccentricity bearing capacity of the LACFT column.

Table 4 Ultimate bearing capacity for LACFT columns for L/D = (3, 7 and 14)

Columns	Test mean	AISC-LRFD 1999		DBJ13-51 2003		CECS 28:90 1990	
	$N_u(kN)$	$N(kN)$	$N/N_u$	$N(kN)$	$N/N_u$	$N(kN)$	$N/N_u$
A1-3-a,b,c	683.82	325.70	0.476	555.82	0.813	668.334	0.977
A2-3-a,b,c	559.73	247.35	0.442	447.97	0.800	531.976	0.95
A3-3-a,b,c	422.02	181.77	0.431	347.07	0.822	408.177	0.967
B1-3-a,b,c	743.43	357.69	0.481	598.97	0.806	730.92	0.983
B2-3-a,b,c	612.77	274.97	0.449	481.78	0.786	581.391	0.949
B3-3-a,b,c	445.86	204.15	0.458	372.58	0.836	443.667	0.995
A1-7-a,b,c	588.93	323.45	0.549	494.65	0.84	534.89	0.908
A2-7-a,b,c	451.37	246.06	0.545	394.15	0.873	426.15	0.944
A3-7-a,b,c	330.66	181.07	0.548	302.53	0.915	326.57	0.988
B1-7-a,b,c	622.99	315.28	0.506	406.66	0.653	425.03	0.682
B2-7-a,b,c	487.78	241.30	0.495	321.98	0.660	338.62	0.694
B3-7-a,b,c	373.11	178.48	0.478	246.54	0.661	259.49	0.695
A1-14-a,b,c	530.29	354.92	0.669	537.22	1.013	585.26	1.104
A2-14-a,b,c	411.4	273.33	0.664	428.68	1.042	465.62	1.132
A3-14-a,b,c	311.32	203.25	0.653	329.46	1.058	356.35	1.145
B1-14-a,b,c	584.49	344.87	0.590	445.58	0.762	465.06	0.796
B2-14-a,b,c	457.3	267.33	0.585	354.33	0.775	369.99	0.809
B3-14-a,b,c	348.05	199.91	0.574	272.41	0.783	283.16	0.814
Average			0.533		0.828		0.919
S.D			0.077		0.119		0.143

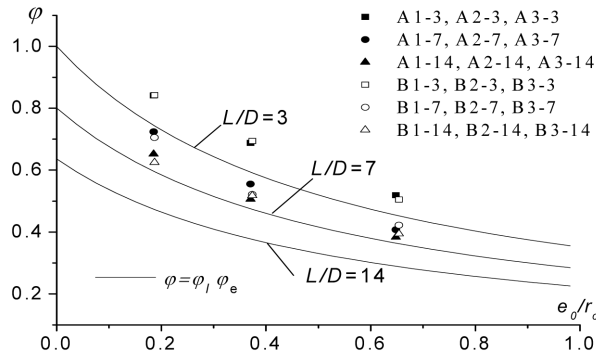


Fig. 10 strength reduction factor versus eccentric ratio curves

By comparing the three slenderness ratios (L/D) 3,7 and 14; it was found from Fig. 10 that, strength reduction factor  $\phi$  of each specimen is gradually decreased along with the increasing eccentric ratio as well as this factor was compared with strength reduction factor of CFT and illustrated in the same figure. Fig. 10 has shown  $\phi$  data points of LACFT distributed above the strength reduction factor of CFT data points versus eccentric ratio. Therefore, it was clear that for specimens under similar circumstances but different concrete type (LACFT or CFT), strength reduction factor of LACFT column is higher than the CFT one.

## 5. Parametric study and analytical models

Based on the results of the experimental work done by a number of researchers that stated in the web site: <http://web.ukonline.co.uk/asccs2> (A database of over 800 tests on concrete-filled steel tube prepared by C. Douglass Goode); the parametric study which includes a wide range of aspect ratio ( $10 \leq D/t \leq 100$ ), concrete uniaxial unconfined compressive strengths ( $f_c = 2$  to 9 ksi), length to width ratios ( $L/D = 3$  to 25) and steel normal yield stresses ( $f_y = 30$  to 70 ksi). The effect of these parameters on the overall response as well as the behavior of individual component element is presented in this section. The results of this study are used to develop analytical models which can express the different aspects of response with considering effect of different parameters. To determine the constant parameters in each analytical model nonlinear curve fitting algorithm is employed. The parameters are iteratively adjusted to minimize a goodness of fit merit function. The analysis is successful when the coefficient of determination ( $R^2$ ) remains constant for five consecutive iterations.

### 5.1. Maximum compressive strength of concrete core

Based on the results obtained relating confinement ratio ( $\xi = f_{max}/f_c$ ) and aspect ratio and between ( $\xi$ ) and ( $f_c$ ). Empirical formulas are developed to determine the maximum confined compressive strength of concrete core, and can be expressed as

$$f_{max} = f_c \times \left( 1 + \frac{0.08 + \frac{9}{f_c^{(1.5)}} - 16.8 \times e^{(-f_c)}}{1 + \frac{D/t}{\rho}} \right) \quad (1)$$

Where ( $D/t$ ) is the aspect ratio and ( $\rho$ ) is empirical parameter that can be expressed in terms of ( $f_c$ ) as

$$\rho = -22 + \frac{1175}{f_c^{(1.5)}} - 1300 \times e^{(-f_c)} \quad (2)$$

As a result, with the knowledge of ( $f_c$ ) and thickness of steel tube ( $t$ ), the compressive strength of concrete core can be accurately calculated.

### 5.2. Maximum compressive stress in steel tube

In this section two empirical equations obtained as a result of studying the effect of ( $D/t$ ) and ( $L/D$ ) ratios on the maximum load carrying capacity of steel tubes in circular CFT columns. This investigation showed that steel tube under biaxial state of stress exhibits a lower yield stress. In the case of short columns, the level of decrease in yield stress depends mainly on ( $D/t$ ) ratio and it is independent of ( $f_y$ ) of steel tube. It is also found that, the decrease in steel tube yield stress ( $f_{sy}$ ) compared to its ( $f_y$ ) is more significant in columns with higher aspect ratio and decrease to 85% of the normal yield stress. Hence a reduction factor ( $\beta_{D/t}$ ) is proposed and defined as

$$\beta_{D/t} = 1.08 \times 0.999^{(D/t)} \times \left( \frac{D}{t} \right)^{(-0.045)} \quad (3)$$

The second parameter which has significant effect on the maximum load carrying capacity of CFT columns is  $(L/D)$ . It's found that, the level of decrease in the maximum stress is more significant in longer columns. However, the degree of reduction is constant for shorter columns up to the limit of  $\frac{L}{D} \leq 10$ . The reduction factor of steel tube due to the effect of length-width ratio ( $\beta_{L/D}$ ) is proposed and defined as

$$\beta_{L/D} = \frac{0.97}{1 - 0.003 \times L/D + 0.0004 \times (L/D)^2} \quad (4)$$

### 5.3. Ultimate load carrying capacity of axially loaded CFT columns

With the knowledge of maximum compressive stresses in the concrete core and steel tube, the ultimate load carrying capacity of CFT columns can be obtained easily by adding the maximum capacity of the concrete core and steel tube. Hence the maximum axial capacity of CFT columns ( $N_{CFT}$ ) can be calculated as

$$N_{CFT} = A_c \times f_{\max} + f_{sy} \times A_s \quad (5)$$

Where,

$$f_{sy} = \beta_{D/t} \times \beta_{L/D} \times f_y \quad (6)$$

In which ( $\beta_{D/t}$ ) and ( $\beta_{L/D}$ ) are reduction factors indicating the effect of aspect ratio and length-width ratio respectively. ( $A_s$ ) and ( $f_y$ ) are the cross sectional area and normal yield stress of steel tube, respectively. ( $A_c$ ) and ( $f_{\max}$ ) are cross sectional area and maximum confined compressive stress of concrete core, respectively. The proposed model is compared with numerous experimental data (Kloppel and Goder 1957, Chapman and Neogi 1964, Furlong 1967) to predict ( $N_{CFT}$ ) of CFT columns under axial load, Fig. 11 present the results of this comparison.

## 6. Modification for AISC-LRFD equation

Two empirical coefficients are proposed to Modify AISC-LRFD code equation to take into account the effect of concrete confinement on the axial load capacity of CFTs columns. A revised equation is proposed as follows:

The squash load is given by

$$P_n = A_s \times f_y + 0.85 \times A_c \times f_c \quad (7)$$

For composite columns

$$\frac{P_n}{A_s} = F_{my} = f_y + 0.85 \times f_c \times \frac{A_c}{A_s} \quad (8)$$

Also

$$E_m = E_s + 0.4 \times E_c \times \left( \frac{A_c}{A_s} \right) \quad (9)$$

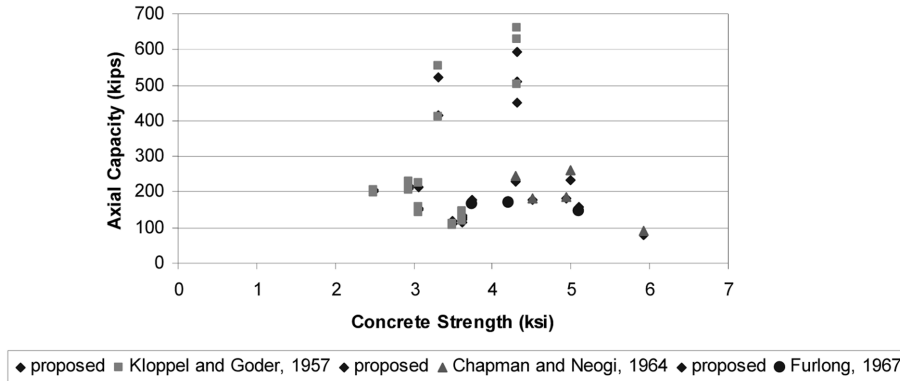


Fig. 11 Comparison of proposed model and experimental results

Where  $E_s$  and  $E_c$  are the modulus of steel and concrete respectively.

$$\lambda_c = 0.658 \lambda_c^2 \times F_{my} \tag{10}$$

$$F_{cr} = 0.658 \lambda_c^2 \times F_{my} \tag{11}$$

Nominal strength  $P_n$  can be calculated as

$$P_n = A_s \times F_{cr} \tag{12}$$

To consider the confinement effect on concrete core it is proposed to replace both ( $f_c$ ) and ( $f_y$ ) in equation (8) by equation (1) ( $f_{max}$ ) and equation (6) ( $f_{sy}$ ) respectively as shown in equation (13).

$$F_{my} = f_{sy} + 0.85 \times f_{max} \times \frac{A_c}{A_s} \tag{13}$$

Table 5 presents the effect of the proposed modification on predicting axial strength of CFTs columns under axial loading.

### 7. Conclusions

The following observations and conclusions are made based on the limited test results described in this paper.

1. Eccentricity ratio is a significant parameter to the mechanical properties of LACFT columns. Where the greater the eccentricity ratio, the less the ultimate bearing capacity, therefore the influence of large eccentricity; the bearing capacity and rigidity decreased, while the ductility performance effectively improved.
2. The steel's ratio influence on the specimen's bearing capacity performance can be described as; the greater the steel ratio, the greater the ascending slope of the curves, as well as increased the

Table 5 Effects of confinement factor in LRFD 1999

D	t (in)	L	Actual capacity	LRFD 1999	$N_u / N_{test}$	Modified LRFD 1999	$N_{um} / N_{test}$
			$N_{test}$ (kips)	$N_u$ (kips)		$N_{um}$ (kips)	
6.1	0.1	24.8	213.2471	138.2688	0.6484	191.1716	0.8965
6.5	0.1	24.8	201.4716	138.2688	0.6863	197.4416	0.9799
6.5	0.1	24.8	210.6775	136.0612	0.6458	197.4416	0.9372
6.5	0.1	49.2	178.3477	136.0612	0.7629	190.9445	1.0706
6.5	0.1	49.2	169.3554	136.0612	0.8034	190.9445	1.1275
6.5	0.1	70.3	179.4201	125.8166	0.7012	182.0406	1.0146
6.5	0.1	70.3	160.363	125.8166	0.7846	182.0406	1.1352
6.5	0.1	70.3	165.5021	123.2560	0.7447	173.3026	1.0471
4.5	0.14	18.8	197.6071	123.2560	0.6237	170.458	0.8626
4.5	0.14	18.8	201.4716	118.5755	0.5885	170.458	0.8461
4.5	0.14	36.7	179.6449	118.5755	0.6600	163.5835	0.9106
4.5	0.14	36.7	156.9392	101.4563	0.6465	163.5835	1.0423
4.5	0.14	50.2	179.2042	101.4563	0.5661	155.6064	0.8683
4.5	0.14	50.2	179.8472	101.4563	0.5641	155.6064	0.8652
4.5	0.14	68.1	185.4135	99.2239	0.5352	142.1352	0.7666
4.5	0.14	68.1	173.2108	99.2239	0.5729	142.1352	0.8206
4.5	0.14	18.8	167.8581	99.2239	0.5911	148.8218	0.8866
4.5	0.14	18.8	160.1494	95.1526	0.5941	148.8218	0.9293

$N_u$  = Ultimate strength of axial compression of CFT columns calculated by LRFD 1999.

$N_{um}$  = Ultimate strength of axial compression of CFT columns calculated by modified LRFD 1999.

ultimate bearing capacity.

- The impact of slenderness ratio on the LACFT columns considering different steel ratios and eccentricity distances was investigated and showed that slenderness ratio has great effect on the columns with  $L/D > 3$  but has no or has negligible effect on the columns with  $L/D \leq 3$ . Moreover load versus deformation curves by different slenderness ratio have smaller ascending slope hence lower bearing capacity achieved.
- Depending on the published data it was found that the confinement effect depends on several factors, namely the thickness of the steel tube, slenderness ratio, eccentricity and cross-sectional shape. It was also found steel tube can produce confinement effect on LAC. Moreover, the bond strength in composite sections is significantly affected by the type of concrete. However, it appears that the type of concrete did not influence the load-slip behavior as the feature of load-slip curves for all types of concrete looks similar.
- Comparisons are made with the predicted column strength using the existing codes such as AISC-LRFD (1999), CHN DBJ 13-51-2003 (2003) and CHN CECS 28:90, the calculated bearing capacities of LACFT by AISC-LRFD are underestimated in comparison to that of the test results, while the calculated value of CHN DBJ 13-51-2003 (2003) are applicable with slightly overestimated values for L/D 14, but the values predicted by CHN CECS 28:90 have a good agreement with the experimental results with slightly overestimated values for L/D 14 too.
- For CFTs circular section, the confinement effect was studied and it was found confinement effect of concrete increase the concrete resistance, but at the time reduces the axial resistance of the steel

section.

7. Concrete with a lower unconfined compressive strength exhibits higher confinement ratio than higher strength concrete.
8. An analytical model is proposed to determine the ultimate axial capacity of CFTs columns. It is shown that the proposed model can predict the load carrying capacity of CFTs with a high accuracy and it is easy to use.
9. Two empirical coefficients are proposed to modify AISC-LRFD 1999, to take into account the effect of concrete confinement on the axial load capacity of CFTs. Table 5 shows that the LRFD modified model can predict the axial load capacity of the CFTs with reasonable accuracy.
10. More experimental investigations are needed to setup new formulas which are able to figure out the problem of the design of composite columns fabricated from concrete filled in steel tube.

## References

- AISC-LRFD (1999), American Institute of Steel Construction, "Load and Resistance Factor Design Specification for Structural Steel Buildings Chicago (IL).
- Boyd FP, Cofer WF and McLean D (1995), "Seismic performance of steel-encased concrete column under flexural loading", *ACI Struct. J.*, **92**(3), 355-365.
- Bradford MA (1996), "Design strength of slender concrete-filled rectangular steel tubes", *ACI Struct. J.*, **93**(2), 229-235.
- Bradford MA, Loh HY and Uy B (2002), "Slenderness limits for filled circular steel tubes", *J. Consty. Steel Research*, **58**(2), 243-252.
- CECS 28:90 (1990), Construction Standard Committee of China, "Chinese specification for the design and construction of concrete-filled steel tubular structures", Planning Publishing House of China Beijing. (in Chinese)
- Chapman, J. C., and Neogi, P. K. (1966), "Research on concrete filled tubular columns", Reports, progress to October 31, 1964 and April 30, 1966, Engineering structures laboratories, Civil Engineering, Imperial College, London, England.
- DBJ13-51-2003 (2003), "Technical Specification for Concrete-Filled Steel Tubular Structures", Fuzhou University, Fujian Province. (in Chinese)
- Elchalakani M, Zhao XL and Grzebieta RH (2001), "Concrete-filled circular steel tube subjected to pure bending", *J. Construct. Steel Research*, **57**(11), 1141-1168.
- Elremaily A and Azizinamini A (2002), "Behavior and strength of circular concrete-filled tube columns", *J. Constr. Steel. Res.*, **58**(12), 1567-1591.
- Fujimoto, T., Mukai, A., Nishiyama, I. and Sakino, K. (2004). "Behavior of eccentrically loaded concrete-filled steel tubular columns". *ASCE J. Struct. Eng.*, **130**(2), 203-212.
- Furlong RW (1967), "Strength of steel-encased concrete beam-columns", *ASCE J. Struct. Div.*, **93**(ST5), 113-124.
- GB/T228-2002 (2002), The People's Republic of China National Standard, "Metallic materials at ambient temperature tensile test method Beijing". (in Chinese)
- Ge HB and Usami T(1992), "Strength of concrete-filled thin-walled steel box columns: experiment", *ASCE J. Struct. Eng.*, **118**(1), 3036-3054.
- Ge HB and Usami T (1994), "Strength analysis of concrete-filled thin-walled steel box columns", *J. Construct. Steel Research*, **30**(3), 259-281.
- Hajjar JF, Molodan A and Schiller PH (1998), "A distributed plasticity model for cyclic analysis of concrete-filled steel tube beam-columns and composite frames", *Eng Struct.*, **20**(4-6), 398-412.
- Han linhai and Yang youfu(2004), "Modern concrete filled steel tubular structures," China building industry Press, Beijing. (in Chinese)
- Han LH, Yao GH (2003) "Behavior of concrete-filled hollow structural steel (HSS) columns with preload on the steel tubes". *J. Constr. Steel. Res.*, **59**(12), 1455-1475.
- Han LH and Zhao XL and Tao Z. (2001) "Tests and mechanics model for concrete-filled SHS stub columns,

*The Behavior of Lightweight Aggregate Concrete Filled Steel Tube Columns Under Eccentric Loading*

- columns and beam-columns". *Steel Compos. Struct.*, **1**(1), 51-74.
- Hu H-T, Huang CS, Wu M-H and Wu Y-M (2003), "Nonlinear analysis of axially loaded CFT columns with confinement effect", *ASCE J. Struct. Eng.*, **129**(10), 1322-1329.
- Huang CS, Yeh Y-K, Liu G-Y, Hu H-T, Tsai KC, Weng YT, Wang SH and Wu M-H (2002), "Axial load behavior of stiffened concrete-filled steel columns", *ASCE J. Struct. Eng.*, **128**(9), 1222-1230.
- Hunaiti Y.M. (1996). "Composite action of foamed and lightweight aggregate concrete". *ASCE J. Materials in Civil Eng.*, **8**(3), 111-113.
- Hunaiti *et al.* (2002). "Evaluation of the concrete contribution factor for composite sections with lightweight aggregate concrete under axial compression". *J Pakistan journal of applied sciences.*, **2**(10), 990-999.
- Ji Bohai, Fu Zhongqiu, MA Jinghai, *et al* (2010), "Impact of eccentricity ratio on behavior of lightweight aggregate concrete filled steel tube columns under eccentricity compression". *South East University (Natural Science Edition) J.*, **40**(3), 624-629.
- Kitada T (1998), "Ultimate strength and ductility of state-of-the-art concrete-filled steel bridge piers in Japan", *Eng. Struct.*, **20**(4-6), 347-354.
- Kloppel, V.K. and Goder, W.,(1957) "An investigation of the load carrying capacity of concrete filled-steel tubes and development of design formula", *Der Stahlbau*, **26**(1), 1-10.
- Knowles RB Park R (1969), "Strength of concrete filled steel tubular columns", *ASCE J. Struct. Div.*, **95**(ST12), 2565-2587.
- Liu, Song (2010). "Experimental study of lightweight aggregate concrete under multiaxial stresses". Zhejiang University-Science A, *J. Appl. Phys. & Eng.*, **11**(8), 545-554.
- Mander J. B., Priestley M. J. N., and Park R., (1988). "Theoretical Stress-Strain Model for Confined Concrete" *ASCE J. Struct Eng.*, **114**(8), 1804-1826.
- M. Mouli and H. Khelafi (2007), "Strength of short composite rectangular hollow section columns filled with lightweight aggregate concrete", *J. Eng. Struct.*, (29), 1791-1797.
- O'Shea MD and Bridge RQ (2000), "Design of circular thin-walled concrete filled steel tubes", *ASCE J. Struct. Eng.*, **126**(11), 1295-1303.
- Roeder CW, Cameron B and Brown CB (1999), "Composite action in concrete filled tubes", *ASCE J. Struct. Eng.*, **125**(5), 477-484.
- Schneider SP (1998), "Axial loaded concrete-filled steel tubes", *ASCE J. Struct. Eng.*, **124**(10), 1125-1138.
- Shams M and Saadeghvaziri MA (1997), "State of the art of concrete-filled steel tubular columns", *ACI Struct. J.*, **94**(5), 558-571.
- Shantung Zhong (2003), Concrete filled steel tubular structure, Qinghua University Press, Beijing.
- Sumei Zhang and Yuning Wang (2004), "Failure modes of short columns of high-strength concrete-filled steel tubes", *China Civil Eng. J.*, **37**(9), 1-10.
- Tomii M, Sakino K and Xiao Y. (1988), "Triaxial compressive behavior of concrete confined in circular steel tube". *Trans Jap Concrete Inst J.* (280), 369-76.
- Uy B (2000), "Strength of concrete filled steel box columns incorporating local buckling", *ASCE J. Struct. Eng.*, **126**(3), 341-352.
- Yang Y. F. and Han L. H. (2006), "Experimental behavior of recycled aggregate concrete filled steel tubular columns". *J. Constr. Steel. Res.*, **62**(12) 1310-1324
- Zhang W and Shahrooz BM (1999), "Comparison between ACI and AISC for concrete-filled tubular columns", *ASCE J. Struct. Eng.*, **125**(11), 1213-1223.
- Zuobin Wei and XiliangLiu (1993), "The fundamental function studies of steel tube cover hoop ceramicist concrete", Proceedings of '93 China Steel's steel concrete composite structure Association 4th Annual Meeting, Guangzhou.

**Notation**

$a, b, c, d$	: Coefficients can be calculated from the code CHN DBJ 13-51-2003
$D$	: Column diameter.
$e_o$	: Eccentricity distance.
$f_y$	: Steel yield strength
$f_{ck}$	: Characteristic concrete prism strength.
$L_o = L$	: Column length
$M$	: Bending moment of the columns.
$M_u$	: Ultimate bending moment of the columns.
$N$	: Ultimate strength of the columns.
$N_u = N_o$	: Ultimate strength of axial compression of columns.
$r_c$	: Concrete core radius.
$t$	: Steel tube wall thickness
$\alpha$	: Steel ratio ( $\alpha = A_s / A_c$ )
$\beta_m$	: A coefficient given by the Chinese code (DBJ13-51 2003) in this
$\eta_o$	: A coefficient can be calculated from the code CHN DBJ 13-51-2003
$\varphi$	: Reduction factor ( $\varphi = N / N_u$ ).
$\varphi_b$	: Resistance factor for bending.
$\varphi_c$	: Resistance factor for compression.
$\varphi_e$	: Strength reduction factor due to the eccentricity ratio.
$\varphi_l$	: Strength reduction factor due to the slenderness ratio